Received: 15 January 2021 | Revised: 23 May 2021 | Accepted: 4 June 2021

DOI: 10.1002/qre.2949

SPECIAL ISSUE ARTICLE

WILEY

# Functional regression control chart for monitoring ship $CO_2$ emissions

**Christian Capezza**[1] | **Fabio Centofanti**[1] | **Antonio Lepore**[1] | **Alessandra Menafoglio**[2] | **Biagio Palumbo**[1] | **Simone Vantini**[2]

[1] Department of Industrial Engineering, University of Naples Federico II, Naples, Italy

[2] MOX - Modelling and Scientific Computing, Department of Mathematics, Politecnico di Milano, Milan, Italy

**Correspondence**
Fabio Centofanti, Department of Industrial Engineering, University of Naples Federico II, Naples, Italy.
Email: fabio.centofanti@unina.it

**Abstract**

On modern ships, the quick development in data acquisition technologies is producing data-rich environments where variable measurements are continuously streamed and stored during navigation and thus can be naturally modelled as functional data or profiles. Then, both the $CO_2$ emissions (i.e. the quality characteristic of interest) and the variable profiles that have an impact on them (i.e. the covariates) are called to be explored in the light of the new worldwide and European regulations on the monitoring, reporting and verification of harmful emissions. In this paper, we show an application of the functional regression control chart (FRCC) with the ultimate goal of answering, at the end of each ship voyage, the question: *given the value of the covariates, is the observed $CO_2$ emission profile as expected?* To this aim, the FRCC focuses on the monitoring of residuals obtained from a multivariate functional linear regression of the $CO_2$ emission profiles on the functional covariates. The applicability of the FRCC is demonstrated through a real-case study of a Ro-Pax ship operating in the Mediterranean Sea. The proposed FRCC is also compared with other alternatives available in the literature and its advantages are discussed over some practical examples.

**KEYWORDS**

functional regression, industry 4.0, multivariate functional linear regression, profile monitoring, statistical process monitoring

## 1 | INTRODUCTION

Nowadays, the quick development in the data acquisition (DAQ) technologies is producing data-rich industrial environments where massive amounts of data are available. In particular, a large portion of the ship observational data are complex measurement signals that may be envisaged as reflecting smooth variations of quantities generated by continuous functions defined on an infinite compact domain, that is, as *functional data*. Functional data analysis (FDA) is a thriving area of statistics. For a comprehensive overview, the reader could refer to Ramsay and Silverman,[1] Horvath and Kokoszka[2] and Kokoszka and Reimherr.[3] In this functional data setting, profile monitoring[4] is the name of a new branch of statistical process control (SPC) that provides a suite of methods to continuously give a solution to the urging issue of evaluating the stability over time of functional quality characteristics. Recent contributions are Colosimo and Pacella,[5] Grasso et al[6] and Menafoglio et al.[7] As in the classical SPC, where data are scalars, profile control charts have the task of monitoring the functional quality characteristic and of triggering a signal when assignable sources of variations (i.e. special causes) act on it. When this happens, the process is said to be out of control (OC). Otherwise, when only normal sources of variation (i.e. common causes) apply, the process is said to be in control (IC).

Only recently, Centofanti et al[8] introduced the functional regression control chart (FRCC) framework to monitor a functional quality characteristic when this is influenced by one or more functional covariates. In particular, the aim of the FRCC is to improve the monitoring of the quality characteristic by including the information coming from the covariates. In this scenario, if one of these covariates manifests itself with an extreme realization, the quality characteristic may wrongly be judged to be OC, even though it shows perfectly reasonable values given the covariates. Otherwise, there may be situations where the covariates are not extreme and the quality characteristic may wrongly appear IC because the information in the covariates is not used to increase the power of the monitoring.

The FRCC framework is the functional extension of the basic Mandel's idea,[9] where the quality characteristic is monitored after being adjusted for the effect of covariates. That is, the control variable is the residual obtained from a regression of the quality characteristic on the covariates, and the focus is spotted on the residual variability not explained by the knowledge of the observed value of the covariates. In a more direct phrasing, the FRCC answers the question: *given the value of the covariates, is the quality characteristic as expected?* Alternatively, the question could be phrased as: *does the assumed model fit the reality of the quality characteristic?* If the answer is no, then special causes may have occurred that are beyond the information brought by the covariates through the chosen regression model. In particular, in the FRCC framework, the quality characteristic and the covariates are linked through a multiple functional linear regression model (MFLR), where both the response and the explanatory variables can be described by functional data. Recent examples of MFLR model can be found in Palumbo et al,[10] Centofanti et al[11, 12] and Chiou et al.[13] The idea of monitoring model residuals arises also in SPC with autocorrelated data, for example, time series.[14–16] In this setting, residuals from an autoregressive model are used to recover independence of the observations, because conventional control charts are known not to work well if the quality characteristic exhibits even low levels of correlation over time.[17] In the regression control chart idea, residuals are used to adjust the quality characteristic for the information in the covariates.

In recent years, profile monitoring has emerged as an effective technique also in the field of maritime transport where the issue of $CO_2$ emission monitoring is becoming of paramount importance.[8, 18, 19] Indeed, in view of climate change and global warming crises, the maritime transport industry is currently facing new challenges related to $CO_2$ emissions. Indeed, the Marine Environment Protection Committee of the International Maritime Organization[20–22] has urged shipping companies to set up a framework for the monitoring, reporting and verification (MRV) of $CO_2$ emissions based on fuel consumption. In the face of these regulations, shipping companies are updating DAQ systems on their fleets, enabling large volumes of observational data to be automatically streamed and transferred to a remote server, bypassing human intervention. A large proportion of these data can be modelled as functional data, thus representing a new challenge for FDA and related SPC methods in this area. The DAQ system installed on modern ships facilitates in fact the collection of functional data related to $CO_2$ emissions as well as to other functional covariates affecting them, which include the speed of the ship, engine variables such as the propeller pitch variables, environmental variables that describe the wind and sea conditions or the cumulative navigation time (we refer to Section 2.2 for more details on the variables considered in this work). However, most of the approaches that have already appeared in maritime literature[23–25] do not take advantage of the potential help to managerial decision making represented by the modelling of the entire voyage profiles acquired and usually compress information in one or more scalar features extracted from them. In this setting, a recurrent request posed by maritime engineers is related to the $CO_2$ emissions corresponding to the given values of other recorded covariates. That is, they want to assess if $CO_2$ emissions are coherent with the values of the covariates, in order to identify unexpected behaviours and take corrective measures. Engineers are less concerned in identifying $CO_2$ emission profiles that are extreme with respect to their marginal distribution, if this can be explained by some extreme value in the covariates. They are rather interested in $CO_2$ emission profiles that are not consistent with covariates affecting them because, for example, they can reveal anomalous ship performance.

The FRCC can be used to meet this engineering need. In this paper, we propose to use the FRCC to monitor ship $CO_2$ emissions throughout each voyage, in order to identify special causes, at given values recorded by functional covariates. Specifically, we consider a particular implementation of the FRCC framework, where the functional quality characteristic, hereinafter referred to also as response, and the functional covariates are related through the multivariate functional linear regression (MFLR) model. In this paper, the MFLR model is estimated based on the multivariate functional principal components analysis (FPCA).[13, 26] Then, studentized residuals are monitored through the simultaneous application of

**TABLE 1** Technical features of the considered Ro-Pax ship

| Features | Value |
|---|---|
| Gross tonnage | 32,728 |
| Length | 203.9 m |
| Beam | 25 m |
| Draft | 6.8 m |
| Maximum power for propulsion | 46,080 kW |
| Maximum speed | 28.9 knots |

the Hotelling's $T^2$ and the squared prediction error (SPE) control charts.[4–6, 27] In this paper, the FRCC framework is used both *retrospectively*, as an aid to the practitioner to determine the IC state of the process under study and to identify an IC reference sample (Phase I), and, *prospectively* to monitor any departure from the IC state at future voyages (Phase II). The applicability of the FRCC is demonstrated through a real-case study of a Ro-Pax ship operating in the Mediterranean Sea, courtesy of the shipping company Grimaldi group.

This work does not directly aim at a real-time feedback control, that is, in the online monitoring and immediate actions during an ongoing voyage. The FRCC framework is indeed used to signal OC voyages once they are completed, as $T^2$ and $SPE$ monitoring statistics are going to be calculated on the entire profiles. Instead, the proposed FRCC focuses on tracking automatically (and possibly the whole fleet) the future OC signals, or patterns and trends that may identify, for example, engine malfunctioning, the need for hull cleaning or for any other energy efficiency initiative. Even though no action could be taken during an ongoing voyage, we believe this paper motivates the use of a functional data approach as the FRCC can be indeed used by shipping companies to evaluate, at the end of a voyage, if the observed $CO_2$ emission profile is anomalous, given the value of the observed covariates. This information can help to prevent and disguise possible problems in future voyages, or to schedule maintenance operations.

The paper is structured as follows. In Section 2, the structure of the data and technological details of the ship equipment are provided for the real-case study at hand. In Section 3, the main materials and methods behind the particular implementation of the FRCC framework are summarized. In Section 4, by means of the real-case study mentioned before, the FRCC is practically applied to monitor $CO_2$ emissions and compared with alternative methods already appeared in the SPC literature. In Section 5, we draw conclusions. All computations and plots have been obtained using the software environment R.[28]

## 2 | TECHNOLOGICAL BACKGROUND AND DATA STRUCTURE

For confidentiality reasons, in what follows we omit the name of the ship considered in the real-case study. However, to give an idea of the ship type, in Section 2.1, we provide its main technical features. Whereas, in Section 2.2, we describe in detail all the variables and the data used for the analysis.

### 2.1 | Technical features

The main technical features of the ship are illustrated in Table 1. The considered ship is characterized by two engine sets, each consisting of two main diesel engines for propulsion Wärtsilä, Type 16ZAV40S, four-stroke, with a maximum continuous rating of 11,520 kW at 510 revolutions per minute (rpm) and by two variable pitch propellers and a shaft generator for electric power supply. The main engine power is used both for propulsion and electrical generation through the shaft generators, which are themselves keyed on a gearbox. The gearbox has two fast inlet shafts powered by the engine shaft, a slow outlet shaft for the propeller and a faster one to which the shaft alternator is connected. The gear ratio between the engine shaft and the propeller shaft is equal to 3.24, whereas the gear ratio between the engine shaft and the shaft alternator is equal to 0.32. The main diesel engine can be powered by three types of fuel with different percentage of sulphur (S) content in order to be compliant with the regulation in force on the geographical area to be sailed: heavy fuel oil, very low sulphur fuel oil ($\leq 0.5\%$ $S$), ultra-low sulphur fuel oil or marine gas oil ($\leq 0.1\%$ $S$). The electrical power supply of the ship consists of three diesel generators (1840 kVA, 690 V), two shaft generators (2100 kVA, 690 V) and one emergency diesel generator (480 kVA). The main engines can supply power in two different modes, at fixed rpm (constant mode) or at variable rpm (combined mode). In the constant mode, shaft generators can be used to supply electric power, even though the maximum speed cannot be reached because speed variations are only possible by changing the pitch of the propellers. Whereas, in the combined mode, the ship speed can be regulated by increasing both pitch propeller and engine rpm, but, vice versa, the possibility to engage the shaft generator is lost.

## 2.2 Data description

Data come from a DAQ system installed on the ship that are transmitted to the cloud with different frequencies varying from 2 to 5 min. The data refer to a specific route, that is, each profile in the data set corresponds to a voyage of the ship and all voyages have the same departure and arrival ports. A period of 11 consecutive months following a dry-dock operation on the ship is considered. Voyages in the first nine months (i.e. from the beginning of February 2020 to the end of October 2020) are used in Phase I, that is, to identify a reference data set, estimate the model and control chart limits. Voyages in the last 2 months (i.e. from the end of October 2020 to the end of December 2020) are used in Phase II to show the performance of the FRCC on monitoring new voyages. We start with a data set of 190 voyages for the Phase I (Section 4.1); then we remove outliers as described in Section 4.1.2 and we end up with a reference data set of 169 voyages; finally, we consider 22 voyages for the Phase II (Section 4.2).

Note that the data refer to the navigation phase. More specifically, the navigation phase begins with the finished with engine order (when the ship leaves the departure port) and ends with the stand by engine order (when the ship enters the arrival port). Moreover, we need to identify an adequate functional domain for each voyage. Even if time is naturally suitable as a functional domain, total travel time can vary from voyage to voyage. Therefore, we prefer to use the fraction of distance traveled over the voyage as the common domain (0,1) of the data.

All the signals acquired by the DAQ system are summarized into several variables that we describe here to select later the functional covariates and response considered in the MFLR model. The ship is tracked by its global positioning system (GPS), which provides longitude and latitude coordinates. The course over ground (COG) is the actual direction of progress of a vessel, between two points, with respect to the surface of the earth, measured in degrees. The sailed distance over ground (SDOG) is the distance travelled by the vessel between two points, measured in nautic miles (NM), calculated from the GPS sensor through the Haversine formula. The speed over ground (SOG) is measured in knots (kn) and is the ratio between SDOG and the sailing time, measured in hours. The propeller pitch (P) is measured in degrees and represents the angle between the intersection of the chord line of the blade section and a plane normal to the propeller axis. An anemometer sensor provides data about the true speed ($V$), measured in knots, and direction ($\psi$), measured in degrees, of the wind. The latter is obtained as the difference between the true wind angle in earth system and the COG. Additional information on the wind variables can be found on Bocchetti et al.[25] From the two anemometer variables, the longitudinal component of the wind is calculated as $V \cos \psi$, while the transversal component is calculated as $|V \sin \psi|$. Note that a positive (respectively, negative) longitudinal component of the wind means that the wind blows from stern (respectively, bow). Moreover, a data fusion process also allows the integration of marine data into the data set, that is, weather forecasts about the sea state furnished by private held weather service provider. The sea state is characterized by the provider through the typical parameters, namely, height and period, used to model waves that, in turn, are roughly divided into two components: wind-driven waves, or simply waves (generated by the immediate local wind) and swell (generated by distant weather systems and usually having larger period). In particular, the height, measured in meters, is defined as the vertical distance from wave crest to wave trough; whereas, the period, measured in seconds, represents the time between successive crests of a train of waves passing a fixed point in a ship, at a fixed angle of encounter.[29] Regarding the $CO_2$ measurement, MRV regulation proposes direct and indirect methods. The direct method determines the amount of $CO_2$ emitted measuring the flow of these emissions passing in exhaust gas funnels. Instead, the indirect method calculates the $CO_2$ emissions based on the fuel consumption. The direct method is based on the determination of $CO_2$ emitted that flow in exhaust gas stacks based on the measurement of the $CO_2$ in the exhaust gas and the measurement of the volume of the exhaust gas flow per unit of time. This method is very sensitive to the calibration and the uncertainty related to the measurement devices. Whereas, the class of indirect method calculates $CO_2$ emissions as a product of the whole amount of fuel consumption of the main and auxiliary engines, boilers, gas turbines and inert gas generators times the so-called *emission factor*, which is calculated as the average emission rate of a greenhouse gas (GHG) relative to the activity data of a source stream, assuming complete oxidation for combustion and complete conversion for all other chemical reactions. In this paper, we use the indirect method and we focus on the main engines only.

In what follows, we list the functional variables chosen for the analysis in this work that are obtained from the signals acquired by the DAQ system. The functional response is the signal corresponding to the $CO_2$ emissions per hour along the

**TABLE 2** Functional covariates used in the MFLR

| | Variable name | Unit of measurement |
|---|---|---|
| 1 | Speed over ground (SOG) | kn |
| 2 | Propeller pitch 1 | degrees |
| 3 | Propeller pitch 2 | degrees |
| 4 | Swell height | m |
| 5 | Wave period | s |
| 6 | Wave height | m |
| 7 | Longitudinal wind component | kn |
| 8 | Transverse wind component | kn |
| 9 | Navigation time | h/(NM[%]) |

*Note*: For confidentiality reasons, *y*-axis labels are omitted.

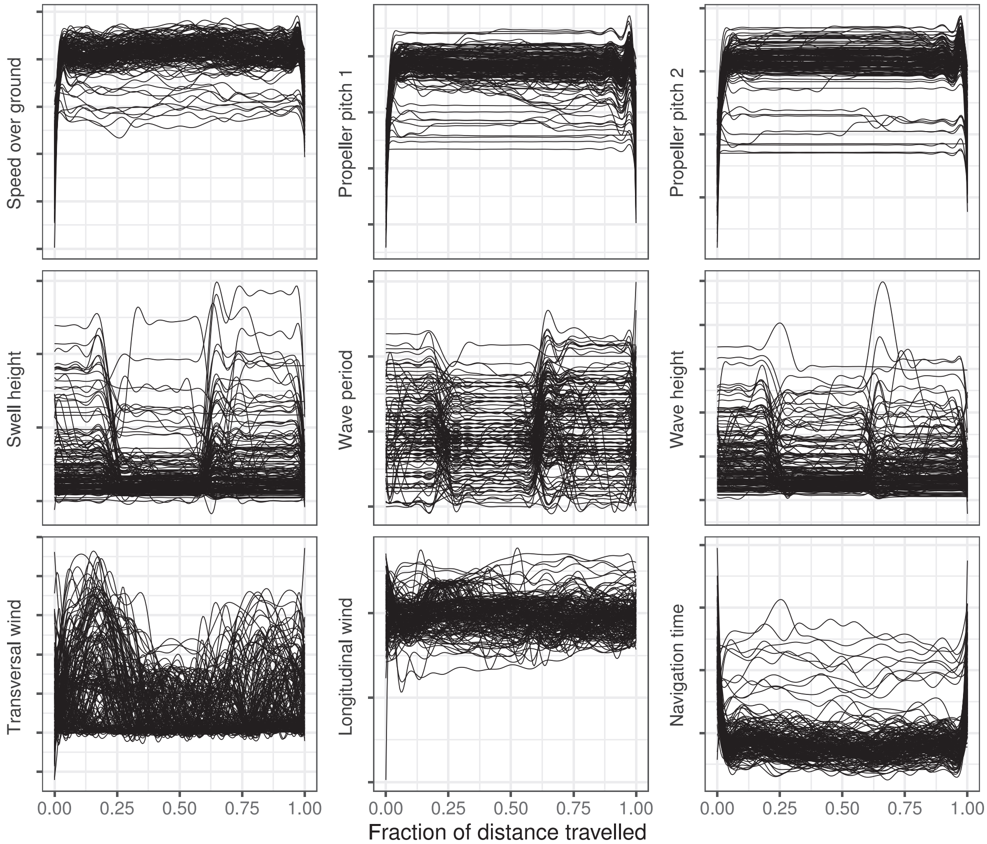


**FIGURE 1** Functional covariates in the reference data set

entire voyage. In order to select functional covariates among the available signals, a very long preliminary investigation was carried out to identify the covariates that could better explain the $CO_2$ emissions. However, in practice, many signals that could have played the role of covariates were not able to be measured accurately. The intersection between the set of candidate and truly measurable covariates was finally identified after an intensive exchange of information and experience with marine engineers, shipping managers and operators. The following nine functional covariates have been identified, which are, thus, assumed as a characterization of the ship operational conditions: SOG, left propeller pitch, right propeller pitch, transversal and longitudinal component of the wind, wave height, wave period, swell height and derivative of the cumulative navigation time. Table 2 reports the complete list of the functional covariates considered in this work.

Moreover, Figures 1 and 2 show the profiles of covariates and response, respectively, included in the reference data set used for model building and control chart limits estimation. In Section 4, we describe with more details how smooth profiles are obtained from the discrete observations acquired by the DAQ system over time, with 2–5 min frequency.

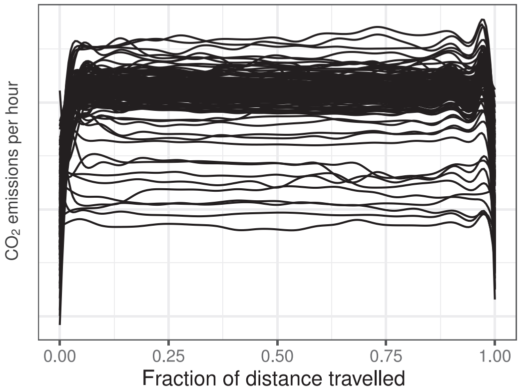


**FIGURE 2** Functional response in the reference data set. For confidentiality reasons, $y$-axis labels are omitted

## 3 METHODOLOGY

The FRCC is a general framework for profile monitoring that can be divided into three main steps.[8] First, (i) define an MFLR model which links the functional response variable $\tilde{Y}$, defined on the compact domain $\mathcal{T}$ and a vector $\tilde{\boldsymbol{X}}$ of random functional covariates $\tilde{X}_1, \dots, \tilde{X}_p$, defined on the compact domain $\mathcal{S}$. Secondly, (ii) define the estimation method of the chosen model and thirdly, (iii) define the monitoring strategy of the functional residual, which is defined as the difference between the fitted value and $\tilde{Y}$. In what follows, we assume that $\tilde{X}_1, \dots, \tilde{X}_p$ and $\tilde{Y}$ have smooth realizations in $L^2(\mathcal{S})$ and $L^2(\mathcal{T})$, that is, the Hilbert spaces of square integrable functions defined on $\mathcal{S}, \mathcal{T} \subset \mathbb{R}$.

A specific implementation of the FRCC can be obtained by assuming for the step (i) the following MFLR model:

$$Y(t) = \int_{\mathcal{S}} (\boldsymbol{\beta}(s,t))^T \mathbf{X}(s) ds + \varepsilon(t) \quad t \in \mathcal{T}, \tag{1}$$

where $Y$ and $\boldsymbol{X}$ are the standardized versions of $\tilde{Y}$ and $\tilde{\boldsymbol{X}}$, obtained through the transformation approach of Chiou et al.[13] The regression coefficient $\boldsymbol{\beta} = (\beta_1, \dots, \beta_p)^T$, is a vector where $\beta_i$'s are square integrable bivariate functions defined on the closed interval $\mathcal{S} \times \mathcal{T}$, and the random error function $\varepsilon$ has zero mean and variance function $v_\varepsilon^2$, and is independent of $\boldsymbol{X}$.

For the step (ii), we use an estimation method based on the multivariate Karhunen–Loève's Theorem.[30] In particular, we assume that the standardized covariate and response variables can be represented as follows:

$$\mathbf{X} = \sum_{i=1}^{\infty} \xi_i^X \boldsymbol{\psi}_i^X \quad Y = \sum_{i=1}^{\infty} \xi_i^Y \psi_i^Y, \tag{2}$$

where $\boldsymbol{\psi}_i^X = (\psi_{i1}^X, \dots, \psi_{ip}^X)^T$ and $\psi_i^Y$ are *principal components* (PCs). PCs are defined as the eigenfunctions of the covariance operator of the standardized covariates and response variable corresponding to the eigenvalues $\lambda_i^X$ and $\lambda_i^Y$ in descending order, respectively. The *scores* $\xi_i^X = \sum_{j=1}^p \int_{\mathcal{S}} X_j(s)\psi_{ij}^X(s)ds$ and $\xi_i^Y = \int_{\mathcal{T}} Y(t)\psi_i^Y(t)dt$ are such that $\mathrm{E}(\xi_i^X) = 0$, $\mathrm{E}(\xi_i^X \xi_j^X) = \lambda_i^X \delta_{ij}$ and $\mathrm{E}(\xi_i^Y) = 0$, $\mathrm{E}(\xi_i^Y \xi_j^Y) = \lambda_i^Y \delta_{ij}$, with $\delta_{ij}$ the Kronecker delta. As demonstrated in Chiou et al,[31] the regression coefficient can be then expressed as follows:

$$\boldsymbol{\beta}(s,t) = \sum_{i,j=1}^{\infty} \frac{\mathrm{E}\left(\xi_i^X \xi_j^Y\right)}{\lambda_i^X} \boldsymbol{\psi}_i^X(s)\psi_j^Y(t) \quad s \in \mathcal{S}, t \in \mathcal{T}. \tag{3}$$

An estimator of $\beta(s,t)$ can be readily obtained by considering the truncated version of Equation (3), that is

$$\boldsymbol{\beta}_{LM}(s,t) = \sum_{i=1}^{L} \sum_{j=1}^{M} b_{ij} \boldsymbol{\psi}_i^X(s)\psi_j^Y(t) \quad s \in \mathcal{S}, t \in \mathcal{T}, \tag{4}$$

with $b_{ij} = \mathrm{E}(\xi_i^X \xi_j^Y)/\lambda_i^X$, and $L, M < \infty$. Plugging Equation (4) into Equation (1), due to the orthonormality of the PCs $\boldsymbol{\psi}_i^X$ and $\psi_i^Y$, we obtain

$$\boldsymbol{\xi}_M^Y = (\boldsymbol{B}_{LM})^T \boldsymbol{\xi}_L^X + \boldsymbol{\epsilon}_M, \tag{5}$$

where $\boldsymbol{\xi}_M^Y = (\xi_1^Y, \dots, \xi_M^Y)^T$, $\boldsymbol{\xi}_L^X = (\xi_1^X, \dots, \xi_L^X)^T$, $\boldsymbol{\epsilon}_M = (\epsilon_1, \dots, \epsilon_M)^T$ and $\boldsymbol{B}_{LM} = \{b_{ij}\}_{i=1,\dots,L, j=1,\dots,M}$, with $\epsilon_i = \int_{\mathcal{T}} \varepsilon(t)\psi_i^Y(t)dt$. Therefore, the problem of estimating $\boldsymbol{\beta}$ reduces to the estimation of the matrix $\boldsymbol{B}_{LM}$, which can be obtained through least squares given $n$ independent realizations $(\tilde{\boldsymbol{X}}_i, \tilde{Y}_i)$ of $(\tilde{\boldsymbol{X}}, \tilde{Y})$. Then, given the least-squares estimator $\hat{\boldsymbol{B}}_{LM}$ of $\boldsymbol{B}_{LM}$, the estimator $\hat{\boldsymbol{\beta}}_{LM}$ of $\boldsymbol{\beta}$ can be calculated as

$$\hat{\boldsymbol{\beta}}_{LM}(s,t) = \left(\hat{\boldsymbol{\psi}}^Y(t)\right)^T \left(\hat{\boldsymbol{B}}_{LM}\right)^T \hat{\boldsymbol{\Psi}}^X(s) \quad s \in \mathcal{S}, t \in \mathcal{T}, \tag{6}$$

where $\hat{\boldsymbol{\psi}}^Y = (\hat{\psi}_1^Y, \dots, \hat{\psi}_M^Y)^T$, $\hat{\boldsymbol{\Psi}}^X = (\hat{\boldsymbol{\psi}}_1^X, \dots, \hat{\boldsymbol{\psi}}_L^X)^T$, with $\hat{\psi}_i^Y$ and $\hat{\boldsymbol{\psi}}_i^X = (\hat{\psi}_{i1}^X, \dots, \hat{\psi}_{ip}^X)^T$ estimators of $\psi_i^Y$ and $\boldsymbol{\psi}_i^X$, respectively. Finally, an estimator $\hat{Y}_{LM}$ of $Y$ is

$$\hat{Y}_{LM} = \sum_{i=1}^{L} \sum_{j=1}^{M} \hat{b}_{ij} \hat{\xi}_i^X \hat{\psi}_j^Y, \tag{7}$$

where $\hat{b}_{ij}$ are the entries of $\hat{\boldsymbol{B}}_{LM}$ and $\hat{\xi}_i^X = \sum_{j=1}^p \int_{\mathcal{S}} X_j(s)\hat{\psi}_{ij}^X(s)ds$.

For the step (iii), we can define the raw functional residual as

$$e(t) = Y(t) - \hat{Y}_{LM}(t) \quad t \in \mathcal{T}. \tag{8}$$

However, by following the remarks in Centofanti et al,[8] we shall better consider a scaled version of it, named *studentized functional residual*, and defined as

$$e_{stu}(t) = \frac{Y(t) - \hat{Y}_{LM}(t)}{\mathrm{Cov}_Y \left(Y - \hat{Y}_{LM}\right)^{1/2}(t)} \quad t \in \mathcal{T}. \tag{9}$$

The residual variance function is estimated as $\widehat{\mathrm{Cov}}_Y(Y - \hat{Y}_{LM})(t) = \hat{v}_\varepsilon^2(t) + \hat{\omega}_{LM}(t,t)$, for $t \in \mathcal{T}$, where $\hat{v}_\varepsilon^2$ is an estimator of $v_\varepsilon^2$ and $\hat{\omega}_{LM}$ is defined as

$$\hat{\omega}_{LM}(s,t) = \mathrm{Cov}\left(\hat{Y}_{LM}\right)(s,t) = \left(\hat{\boldsymbol{\xi}}_L^X\right)^T \left(\hat{\Xi}_{\mathbf{X}}^T \hat{\Xi}_{\mathbf{X}}\right)^{-1} \hat{\boldsymbol{\xi}}_L^X \hat{\boldsymbol{\psi}}_M^Y(s)^T \hat{\boldsymbol{\Sigma}}_{\epsilon_M} \hat{\boldsymbol{\psi}}_M^Y(t) \quad s \in \mathcal{S}, t \in \mathcal{T}, \tag{10}$$

where $\hat{\boldsymbol{\xi}}_L^X$ is the estimator of the score vector $\boldsymbol{\xi}_L^X$ of $\mathbf{X}$, $\hat{\Xi}_{\mathbf{X}}^T \hat{\Xi}_{\mathbf{X}}$ is the estimator of $n\,\mathrm{Cov}(\boldsymbol{\xi}_L^X, \boldsymbol{\xi}_L^X)$, $\hat{\boldsymbol{\psi}}_M^Y$ is the estimator of the vector of the first $M$ eigenfunctions of $Y$, and $\hat{\boldsymbol{\Sigma}}_{\epsilon_M}$ is the estimator of $\mathrm{Cov}(\boldsymbol{\epsilon}_M)$. As stated in Ref. [8], the use of the studentized functional residual, in place of the raw residual, is needed to reduce the effect of covariate mean shifts on the performance of the FRCC to identify OC condition of the quality characteristic, which can be large especially when the coefficient function is poorly estimated. In this case, it can be demonstrated that the interpretation of the FRCC becomes cumbersome, indeed a point falling outside the FRCC control limits could be wrongly assigned to a mean shift in the quality characteristic even though it shows a perfectly reasonable behaviour given the value of the covariates. This is problematic because the aim of the FRCC is to monitor the quality characteristic assigned the value of the covariates, and, thus, if a mean shift in the covariates causes an OC, the chart is saying that the value of quality characteristic disagrees with those of the covariates that, of course, it is not true. In this respect, the studentized functional residual is less influenced by covariate mean shifts than the raw residual. Indeed, the aim of $\mathrm{Cov}_Y(Y - \hat{Y}_{LM})^{1/2}$ is to weight the raw residual on the basis of its uncertainty, such that for an extreme realization of $\boldsymbol{X}$, the residual is heavily scaled. Thus, the probability of the quality characteristic to be judged IC, when no special causes apply to the process, is larger than that corresponding to the raw residual. Note that, for a large sample sizes, consistently with the data set complexity, the studentized functional residual leads to the same results of the raw residual, because in this case it is independent of the values achieved by the covariates. Therefore, the use of studentized residual allows controlling the false alarm rate in presence of covariate mean shifts, which comes at a cost of reducing the power of the FRCC in identifying OCs in the quality characteristic, especially for extreme values of the covariates. However, this behaviour is inevitable because comes from the greater uncertainty in the model estimation originated by a limited number of extreme realizations in the reference sample.

We use a monitoring strategy based on the Hotelling's $T^2$ and the $SPE$ control charts[4, 6 27, 32] applied to $e_{stu}$ in Equation (9). In particular, the studentized functional residual $e_{stu}$ is approximated as

$$e_{stu,K} = \sum_{i=1}^{K} \xi_i^e \psi_i^e, \tag{11}$$

where the scores $\xi_i^e = \int_{\mathcal{T}} e(t)\psi_i^e(t)dt$ and the PCs $\psi_i^e$ are the eigenfunctions corresponding to the eigenvalues $\lambda_i^e$ in descending order of the covariance function of $e_{stu}$. The Hotelling's statistic $T^2$ is obtained as follows:

$$T_e^2 = \boldsymbol{\xi}^e \boldsymbol{\Sigma}_{\xi^e}^{-1} \boldsymbol{\xi}^e, \tag{12}$$

where $\boldsymbol{\Sigma}_{\xi^e} = \text{diag}(\lambda_1^e, \dots, \lambda_K^e)$ is the variance–covariance matrix of $\boldsymbol{\xi}^e = (\xi_1^e, \dots, \xi_K^e)^T$. Note that $T_e^2$ is the squared distance of the projection of $e_{stu}$ from the origin of the space spanned by the PCs standardized for the score variances. Analogously, changes along directions orthogonal to the latter space are monitored by the statistic

$$SPE_e = \int_{\mathcal{T}} \left(e_{stu}(t) - e_{stu,K}(t)\right)^2 dt. \tag{13}$$

The control charts are designed in Phase I by means of a set of $n$ functional studentized residuals $e_{stu,i}$, $i = 1, \dots, n$, obtained by $n$ independent realizations $(\tilde{\boldsymbol{X}}_i, \tilde{Y}_i)$ acquired under IC conditions. Phase I includes also the estimation of the MFLR model unknown parameters, the PCs $\psi_i^e$ and the matrix $\boldsymbol{\Sigma}_{\xi^e}$ (calculated by means of the sample covariance) as well as the estimation of the control limits for both the Hotelling's $T^2$ and the $SPE$ control charts. The latter can be obtained by means of the $(1-\alpha)$-quantiles of the empirical distribution of the two statistics, where $\alpha$ is chosen to control the overall type I error probability. In the monitoring phase (Phase II), the functional studentized residuals of new data are calculated and an alarm signal is issued if at least one of the corresponding $T_e^2$ and $SPE_e$ statistics violates the control limits.

## 4 | RESULTS AND DISCUSSION

In this section, we show the results of the application of the FRCC to the data set described in Section 2.2. In particular, the retrospective and prospective phases, that is, Phase I and Phase II, are described in Section 4.1 and Section 4.2, respectively. Moreover, in Section 4.3, a comparison with simpler monitoring approaches is shown.

We have used the R package `funcharts` to build the FRCC and perform all the analysis shown in this paper. The package is available on CRAN at https://cran.r-project.org/web/packages/funcharts/index.html. Moreover, in the supplementary material we provide an R script and the data to reproduce the results in this paper. Note that the data have been scaled for confidentiality reason.

### 4.1 | Phase I

Phase I comprises the recovery of smooth functional data from the discrete observations for each voyage (Section 4.1.1), the identification of the reference data set of IC voyages (Section 4.1.2) and, the estimation of the MFLR model as described in Section 3 (Section 4.1.3).

#### 4.1.1 | Data smoothing

The first step of the analysis is to get smooth functional data from the discrete observations for each voyage of the ship. We use B-spline basis expansion and penalized least squares to estimate the corresponding basis coefficients. A common

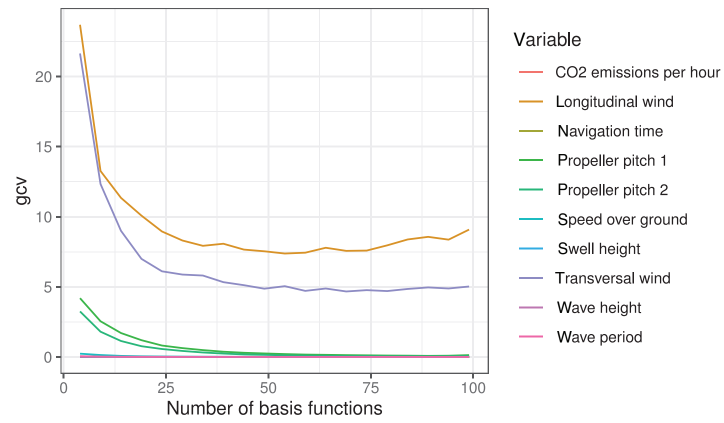


**FIGURE 3** Median, across all voyages in the Phase I data set, of the generalized cross-validation (GCV) error as a function of the number of basis functions, for each functional variable

approach is to set a quite large number of basis functions and then select the optimal smoothing parameter by minimizing the generalized cross-validation (GCV) error.[1] However, the number of available discrete points is above 200 for each voyage and, by following this approach, the GCV criterion leads to choosing the smoothing parameter equal to zero in practice for all functional variables. This is a typical problem of overfitting, as also pointed out by Reiss and Ogden,[33] which show that at finite sample sizes GCV is likely to develop multiple minima and undersmooth. Therefore, we encourage parsimony and achieve regularization by choosing a small, efficient number of basis functions, with the smoothing parameter fixed to a small positive value (i.e. $10^{-10}$) to ensure identifiabilty. In Figure 3, we plot the GCV error against the number of B-spline basis functions. While increasing the number of basis functions reduces the GCV error, we select 25 basis functions for all functional variables as the elbow point of these curves.

### 4.1.2 | Reference data set

Once functional data are obtained, in order to monitor a set of voyages in a considered period, it is necessary to identify a reference data set of previous IC voyages that can be used for model building and estimation of the Hotelling $T^2$ and $SPE$ control chart limits. Starting from an historical data set, any voyage that is not representative of the IC conditions has to be removed from it. Specific Phase I techniques are designed for the problem of eliminating anomalous voyages from the historical data set and generally lead to the construction of control charts with different limits from the ones calculated in Phase II. However, the problem of selecting the best method to perform Phase I is beyond the scope of this paper, which is instead mainly focused on Phase II monitoring. In this paper, we use the same FRCC framework also in Phase I and based on experts' opinion, to establish which voyages are actually considered anomalous and have to be excluded. That is, we first use the historical data set to build the FRCC and estimate the control chart limits, and we plot the FRCC for the same voyages; then, voyages signalled as anomalous are carefully investigated by maritime engineers to understand if special causes occurred; in these cases, voyages are removed from the data set; the process is repeated until the final reference data set is obtained, which contains only voyages considered as IC. Starting from the initial historical data set of 190 voyages, at the end of this iterative process of identifying outliers, detecting anomalies, removing anomalous voyages and refitting the model, we get a reference data set of 169 voyages. Figure 4 shows the FRCC applied to the initial data set. The $x$-axis label indicates the voyage number (VN) and is here intended to be a progressive counting label to denote subsequent voyages in the data set. Moreover, Figure 5 shows some OC studentized residual profiles correctly signalled as anomalous.

### 4.1.3 | Model building

The FRCC relies on the choice of $L$ and $M$ in Equation (4), as well as $K$ in Equation (11). Figure 6 shows the cumulative fraction of variance explained by the functional PCs in the multivariate functional covariates, the functional response and the functional studentized residuals, respectively. Based on the results in Figure 6, we opt for a more parsimonious choice than that suggested in Centofanti et al[8] and set the thresholds for the explained variability in the data as 80%, 95% and

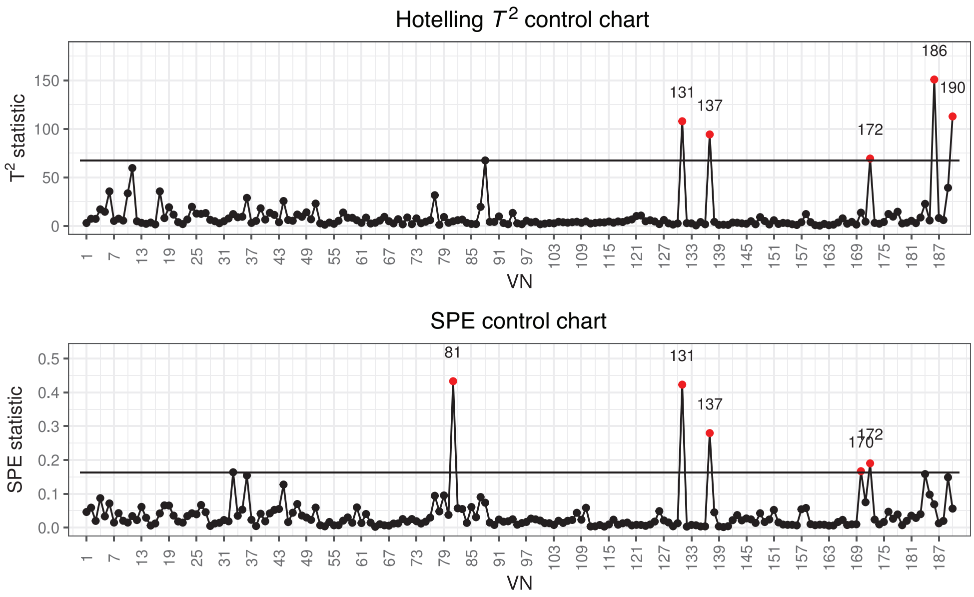


**FIGURE 4** FRCC used for Phase I monitoring on the initial data set of 190 voyages, to remove outliers and define the reference data set

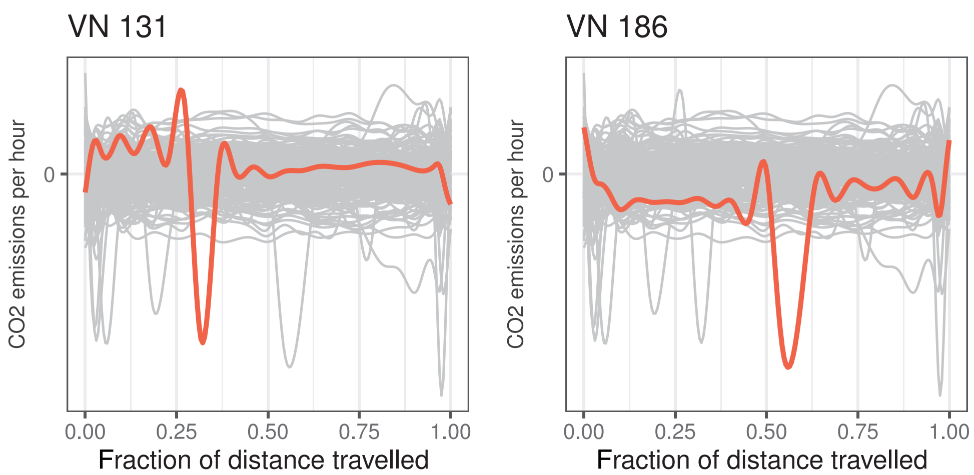


**FIGURE 5** Some functional studentized residuals identified as OC in Phase I, plotted in red against all the other ones in the original Phase I data set, plotted in grey

95%, respectively, that is, we select $L = 7$, $M = 1$ and $K = 8$. The corresponding actual fractions of variance explained are 81%, 96% and 96%.

To allow for a possible interpretation of the selected functional PCs, in Figure 7 we plot the eigenfunctions of the covariance operator of the standardized multivariate functional covariates. Since they all have unit norm, we multiply them by the square root of the corresponding eigenvalues so that profiles with larger norm are PCs that explain a larger fraction of the total variance in the data. It can be readily envisaged that the first PC depends almost entirely on the two propeller pitch variables, the SOG and the navigation time. The latter is negatively correlated with the other variables, and for all these variables, weights are almost constant over the entire functional domain. The second PC strongly depends on the sea state descriptors (swell height, wave height and wave period) and only on the transversal component of the wind. These functional variables all have positive weight, with some parts of the domain showing slightly larger weight than others. The third PC seems to mainly depend on the longitudinal component of the wind alone. In other words, the first PC describes how fast the ship is moving, while the second and third PCs capture two distinct aspects of environmental conditions. Figure 8A shows the first PC (i.e. eigenfunction) of the covariance operator of the standardized functional response, that alone explains most of the variability in the data. This highlights that, after standardization, all

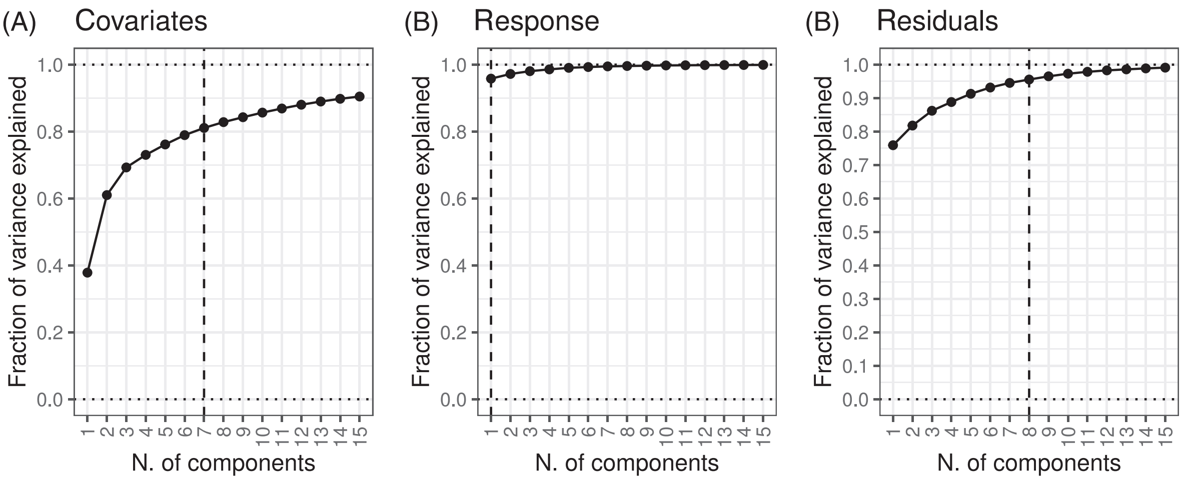


**FIGURE 6** Eigenvalues of the covariance operator of the functional covariates (A), the functional response (B) and the functional studentized residuals (C), estimated on the reference data set. Vertical dashed lines indicate the selected number of components

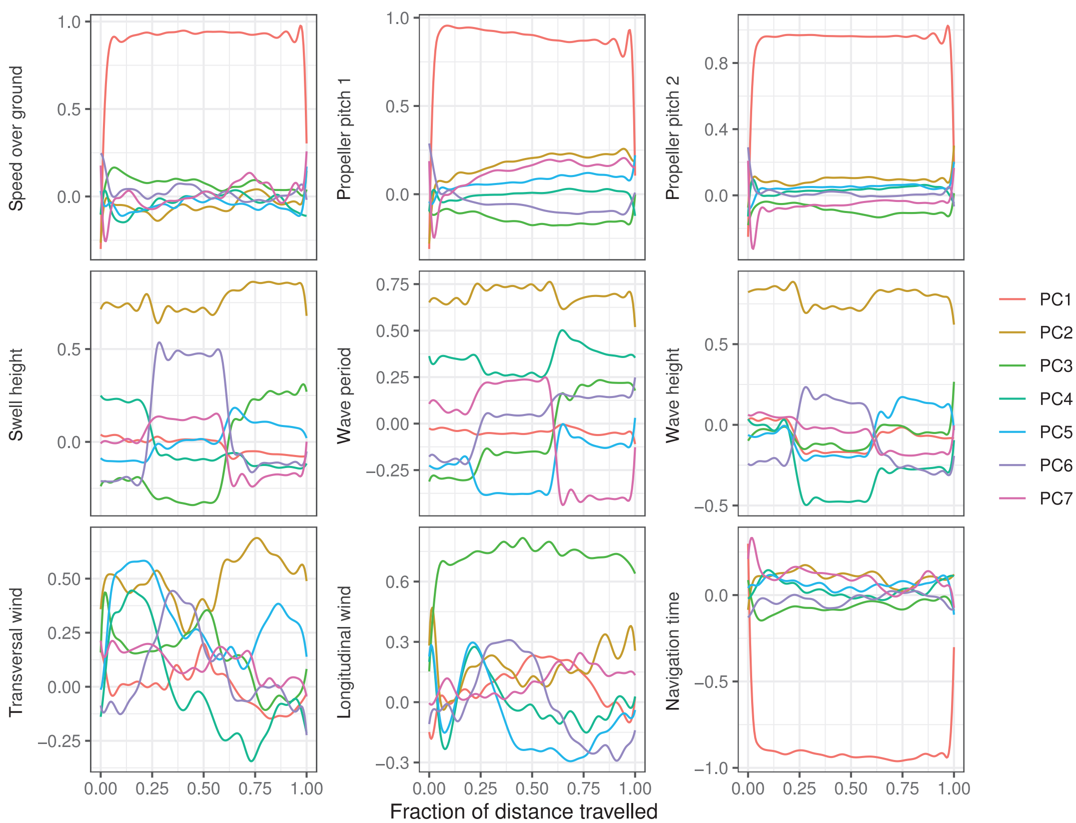


**FIGURE 7** Eigenfunctions of the covariance operator of the functional covariates, estimated on the reference data set

fuel consumption per hour profiles are mostly constant over the entire domain, apart from the beginning and the end of the voyage . Figure 8B shows the eigenfunctions of the covariance operator of the studentized residuals. The first PC depends on the average value over the entire voyage. The second PC accounts for the difference between the first and the second half of the voyage. Whereas, some of the following PCs seem to assign a larger weight to the boundaries of the functional domain, but, however, their interpretation becomes less straightforward.

Figure 9 shows the estimated functional coefficients obtained as in Equation (6). Since the functional response is approximated with a single functional PC, which, in practice, is constant over the entire domain, the functional coefficient shows only vertical bands along the direction of $t$. The most important predictors are those associated with the first and third